Check for updates

Original Research Article

New 5-fluorouracil Anti-tumor Ferric Oxide Nanoparticles Inhibit Cervical Cancer by Regulating the Expression of Nuclear Factor Kappa B

Pharmacognosy Magazine
22(3) 909–917, 2026
© The Author(s) 2025
Article reuse guidelines:
in.sagepub.com/journals-permissions-india
DOI: 10.1177/09731296251396308
journals.sagepub.com/home/phm
Sage

Xiaoyue Zhang[1], Junqin Wang[1], Xiaojuan Shen[1], Yaqin Shen[1], Xiaomei Zhang[1] and Chenlu Zhu[1]

Abstract

Background: 5-Fluorouracil (5-FU) is a classic chemotherapy drug. Iron oxide nanocarriers (Fe_3O_4-NPs) significantly increase 5-FU concentration at tumor sites by enhancing targeting and sustained-release properties, while reducing systemic toxicity.
Objectives: Our research aims to explore the mechanism of the activity of novel 5-FU anti-tumor Fe_3O_4 nanoparticles (NPs) in cervical cancer.
Materials and Methods: Prepare novel 5-FU-Fe_3O_4-NPs, analyze the nanomaterial properties through electron microscopy, the effect of 5-FU-Fe_3O_4-NPs on nuclear factor kappa B (NF-κB) expression was determined by reverse transcription polymerase chain reaction (RT-PCR), and cell proliferation was determined by 3-(4,5-dimethylthiazol-2-yl)-2,5-diphenyltetrazolium bromide (MTT). Flow cytometry and MTT detected cell biological behavior. 5-FU solution (control group) or 5-FU-Fe_3O_4-NPs were injected through the skin to treat skin metastases in nude mice, and the tumor volume was counted, and its size was measured.
Results: The average diameter of the NPs is 310 nm, and 70% of the particles are less than 385 nm, showing strong homogeneity. 5-FU-Fe_3O_4-NPs can inhibit NF-κB signaling molecule, a subunit of NF-κB transcription factor (P65) expression in cervical cancer cells, and the inhibition rate increases with the increase of 5-FU-Fe_3O_4-NPs concentration. 5-FU-Fe_3O_4-NPs can inhibit the increase in cervical cancer cell proliferation. Cell proliferation showed reduced surviving cells in 5-FU-NPs. Mouse cervical cell carcinoma also suggested that 5-FU-Fe_3O_4-NPs can significantly inhibit the growth of tumor cells, and this mechanism is mainly through inhibition of NF-κB expression.
Conclusion: 5-FU-Fe_3O_4-NPs, new anti-tumor NPs, can inhibit cell proliferation and promote apoptosis. 5-FU-Fe_3O_4-NPs, new anti-tumor NPs, can inhibit cell activities. It may slow down the proliferation of cervical cancer by regulating NF-κB signaling and have a significant anti-tumor effect.

Keywords

5-Fluorouracil, Fe_3O_4, nuclear factor kappa B, cervical cancer, proliferation, apoptosis

Received 12 February 2025; **revised** 21 May 2025; **accepted** 18 September 2025

Introduction

The possible mechanism of cervical cancer is due to the inactivation of tumor cell-induced signal transduction. Some studies have also shown that this mechanism involves the generation of a tumor microenvironment through immune regulatory factors, thus limiting the effective immune response of the host (Hull et al., 2020; Parrondo et al., 2010). In addition, nuclear factor kappa B (NF-κB) is highly expressed in various tumors such as prostate, breast, lung, stomach, colon, esophagus, and uterus. Currently, 5-fluorouracil (5-FU) is the main systemic chemotherapy, especially in the treatment of tumor metastasis (Cai et al., 2020; Liu, Wang, et al., 2022). Direct administration of metastatic lesions can quickly absorb 5-FU into the blood circulation, resulting in insufficient local drug dosage in the body. Therefore, given the current situation, it is required to

[1]Department of Obstetrics and Gynecology, Dongtai Hospital of Traditional Chinese Medicine, Yancheng, Jiangsu, China

Corresponding author:
Xiaojuan Shen, Department of Obstetrics and Gynecology, Dongtai Hospital of Traditional Chinese Medicine, No. 6, Beiguan Road, Yancheng, Jiangsu 224200, China.
E-mail: SXJ15151096996@163.com

Creative Commons Non Commercial CC BY-NC: This article is distributed under the terms of the Creative Commons Attribution-NonCommercial 4.0 License (http://www.creativecommons.org/licenses/by-nc/4.0/) which permits non-Commercial use, reproduction and distribution of the work without further permission provided the original work is attributed as specified on the SAGE and Open Access pages (https://us.sagepub.com/en-us/nam/open-access-at-sage).

discover new treatment strategies to achieve better results in the treatment of cervical cancer.

NF-κB signaling regulates cellular functions (Guo et al., 2023; Yu et al., 2018), and its activation has been found in several malignancies, including breast, cutaneous squamous cell carcinoma (cSCC), lung, and female tumors, and is involved in tumor recurrence (Primorac & Musacchio, 2013). In non-small cell lung cancer, signaling through NF-κB has long been considered critical for skin epidermal development and homeostasis, and many studies have confirmed this. Recently, the NF-κB pathway controls the initiation and progression of human papillomavirus (HPV)-driven cSCC (Zhang et al., 2014). The NF-κB signaling pathway regulates cell activities (Hua et al., 2019) and is associated with cervical cancer grade (Chu et al., 2019; Liu, Zhou, et al., 2022). A subunit of the NF-κB transcription factor (P65) is a target of the NF-κB pathway. P65 enters the nucleus after binding and stabilizing to regulate the expression of target genes. P65 is associated with enhanced invasiveness of various cancer types, including cervical cell carcinoma (Grosse et al., 2016; Liu, Fu, et al., 2021).

Nanoparticles (NPs) have received widespread attention from the medical community since the beginning of 1978 (Grigoras, 2017). Polymer microspheres can protect drugs from interference from external factors and reduce the impact on the drug release rate (Rezvantalab et al., 2018). Forming nanospheres by wrapping high molecular polymers can block the interference of hydrophilic groups. Compared with microspheres, NPs have advantages in enhancing target effects and reducing side effects (Klekotko et al., 2015; Lee et al., 2019). New blood vessels within tumors are more permeable to NPs at 400–600 nm (Liu, Wang, et al., 2021). However, the intraperitoneal delivery of NP anti-tumor drugs for the treatment of peritoneal metastasis of cervical cancer has not been extensively studied. In view of this, we first used a new technology to prepare 5-FU NPs and demonstrated the mechanism.

Materials and Methods

5-FU-Fe_3O_4-NPs Preparation

First, add 5-FU-Fe_3O_4-NPs into 80 mL of dichloromethane. Under high shear emulsification conditions, 4 mL of 10% (w/w) NaOH containing 5-FU was mixed to obtain a slightly transparent emulsion. Under strong stirring, drop it into 5-FU solution containing 5% (w/v) polyvinyl alcohol (PVA) for 5 min to acquire a double emulsion (w/o/w) and evaporate using a rotary evaporator. NPs were recovered by centrifugation and then rinsed with the final lyophilized saturated aqueous solution of 5-FU and distilled water.

Evaluate NPs Quality

Evaluate morphological characteristics of NPs. Disperse 1 mg of NPs in 1 mL of water. The NPs suspension was dropped on a glass slide, and the specimen was prepared by fixing it with aldehydes and barium tetroxide (OsO_4) at room temperature, and using 40%, 70%, 90%, and 100% ethanol, the specimen was dehydrated using a dehydrator. Ultrathin sections of biological material are embedded and post-stained with heavy metal salts such as uranium, resulting in the introduction of contrast agents within the sample. After preparation, morphology was studied by scanning electron microscopy (Carl Zeiss [Shanghai] Management Co., Ltd.).

The morphology of exosomes was assessed by transmission electron microscopy (TEM) (JEM-2100, Jeol, Japan).

Encapsulation efficiency was determined by thermogravimetric analysis (STA409 Thermal Analyzer, Germany) at 10 uC/min (under nitrogen) atmosphere.

Disperse 50 mg of 5-FU-Fe_3O_4-NPs in phosphate buffered saline (PBS). Dialyze the solution in a dialysis bag and put it into PBS, seal it, stir and mix well, collect 10 mL samples from the external PBS at specified time intervals, and add an equal amount of fresh PBS. The research mechanism is shown in Figure 1. The average diameter of the NPs determined by dynamic light scattering was 310 nm, and the particle size distribution was concentrated. 70% of the particles were smaller than 385 nm.

Experimental Animals

Mice raised under the same conditions (provided by the Jiangsu University Experimental Animal Center, aged 6–8 weeks) had access to food and water, and were exposed to a 12 h light:12 h dark cycle. Two groups of controls were used. Experimental mice were treated with 5-FU-NPs, and the control group was treated with 5-FU solution. After 8 weeks, skin injection was performed (40 mg/kg). At 14 weeks, collect materials uniformly, use 25 mL of control (50 mg/mL 5-Bru solution) and 800 mL of ethyl acetate, stir

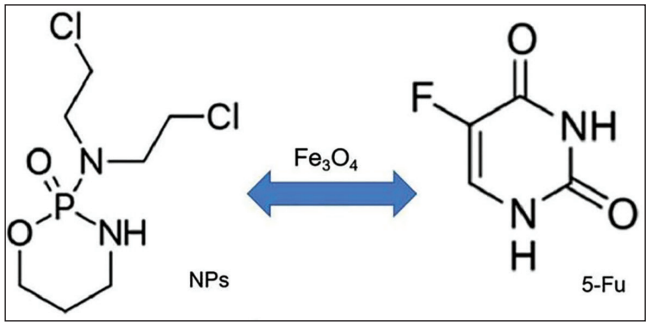


Figure 1. 5-FU-Fe_3O_4-NPs Molecular Schematic.

Note: 5-FU-Fe_3O_4-NPs: 5-Fluorouracil ferric oxide nanoparticles.

for 1 min, centrifuge for 5 min (5,000 rpm), and then filter and precipitate the solution through a filter. Finally, the sample was injected into the high-performance liquid chromatography (HPLC), and the 5-FU concentration was calculated.

Cell Migration Assay

Boyden chambers (8.0 mm pore size) were coated with collagen (10 mg/mL) for migration or Matrigel for invasion, followed by crystal violet staining before observation.

Effect of 5-FU-Fe_3O_4-NPs on Cervical Cancer Cell Transplant Tumors

The principles of animal use follow the guidelines of our hospital's ethics committee. HeLa cells (1×10^5/mouse)/mL were injected into the skin of mice ($n = 5$ mice/group). Starting from the 7th day, 5-fluorouracil sol and 5-FU-Fe_3O_4-NPs were intraperitoneally injected (40 mg/kg) every week. The number of peritoneal nodules with a diameter <1.0 mm or >3.0 mm was counted, and the data were from representative experiments.

Cell Apoptosis

Cells were stained with Annexin V-FITC, PI, or isotype control to measure cell apoptosis by flow cytometry.

Cell Cycle

Cells were fixed, followed by the addition of 10 mg/mL RNase A, 400 mg/mL propidium iodide, and 0.1% Triton-X. Labeled cell DNA content was analyzed using FlowJo.

Immunohistochemical Staining

After treatment, primary antibodies (1:100, Abcam) were applied and then followed by secondary antibody, hematoxylin staining, and post-counterstaining with blue reagent.

Immunofluorescence

After transfection, cells were fixed and permeabilized. After serum blocking, the primary antibody was added overnight, and then the secondary antibody, followed by nuclear counterstaining and observation under a fluorescence microscope.

Analysis of the Effect of Cell Proliferation

Cells were collected at the most vigorous period of cell growth, fixed, permeated, and divided into 96-well plates (1×10^5 cells /200 μL). The culture dish was immersed in PBS containing 1 mmol/l $MgCl_2$, and the non-adherent cells were removed. Then, the adherent cells were measured by the 3-(4,5-dimethylthiazol-2-yl)-2,5-diphenyltetrazolium bromide (MTT) method at 490 nm wavelength. Subsequently, 30 mL MTT (5 mg/mL) was added for 4 h. After incubation, the sample was centrifuged at 2,200× for 5 min. Once the supernatant, 150 mL of dimethyl sulfoxide (DMSO), is added to resolve the crystal, and the optical density (OD) value is measured at 490 nm after 15 min of marking. All experiments were performed four times and repeated twice.

Reverse Transcription Polymerase Chain Reaction (RT-PCR)

RNA was extracted from miRNeasy FFPE using TransScript Green One-Step qRT-PCR SuperMix (Shanghai Thermo Fischer Co., Ltd.). TM microRNA qPCR quantitative kit. With glyceraldehyde-3-phosphate dehydrogenase (GAPDH) as a control, the real-time PCR system (Shanghai Thermo Fisher Co., Ltd.) used total cDNA as the starting material for real-time PCR. Software analysis. Table 1 lists the primers and primer sequences.

Western Blot

The 10% sodium dodecyl sulfate polyacrylamide gel electrophoresis (SDS-PAGE) isolated protein was used. After membrane transfer, it was sealed with 5% skimmed milk. The primary antibody (anti-P65, inhibitor of kappa B alpha [IκBα], diluted at 1:1,000) was incubated at 4°C overnight. The secondary antibody (horseradish peroxidase (HRP)-labeled, diluted at 1:5,000) was incubated for 1 h. After enhanced chemiluminescence (ECL) development, quantitative analysis was performed using Image J.

Statistical Methods

Statistical Package for the Social Sciences (SPSS) processed data, which were displayed as mean ± SD and assessed by Student's t test. $p < .05$ refers to a difference.

Results

Effect of 155-FU-Fe_3O_4-NPs on the Expression of NF-κB

5-FU-Fe_3O_4-NPs may affect NF-κB signaling. To further verify 5-FU-Fe_3O_4-NPs' effect on molecular signaling of cervical cancer cells, NF-κB expression was measured, and it was shown that 5-FU-Fe_3O_4-NPs could inhibit NF-κB signaling molecule P65 expression, and the inhibition rate increased with the increase of 5-FU-Fe_3O_4-NPs concentration ($p < .05$) (Figure 2A). 5-FU-Fe_3O_4-NPs-treated cervical cancer cells showed reduced proliferation ($p < .05$) (Figure 2B).

Table 1. Primer Sequences.

P65 mRNA	F	5′-CTGCAGACCTTGGAGCTTGT-3′
	R	5′-CAGGTCCCGCTTCTTTACCT-3′
GAPDH	F	5′-GAAGGTGAAGGTCGGAGTC-3′
	R	5′-GAAGATGGTGATGGGATTTC-3′

Note: GAPDH: Glyceraldehyde-3-phosphate dehydrogenase; P65: A subunit of NF-κB transcription factor.

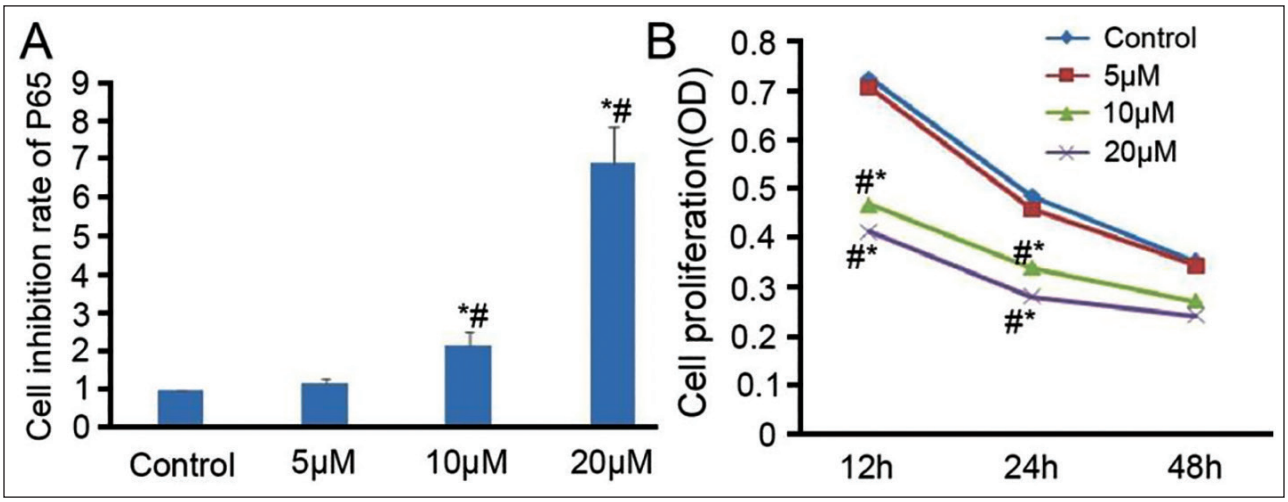


Figure 2. Effect of 5-FU-Fe_3O_4-NPs on the Expression of NF-κB in Cervical Cancer Cells. (A) The Expression of P65 Inhibition Rate was Detected by RT-PCR. (B) The Effect of MTT Detection of 5-FU-Fe_3O_4-NPs on Cell Proliferation of Cervical Cancer Cells was Shown.

Notes: Compared with Control Group, *$p < .05$; Compared with Low Dose Group, #$p < .05$. 5-FU-Fe_3O_4-NPs: 5-Fluorouracil ferric oxide nanoparticles; MTT: 3-(4,5-Dimethylthiazol-2-yl)-2,5-diphenyltetrazolium bromide; NF-κB: Nuclear factor kappa B; P65: A subunit of NF-κB transcription factor; RT-PCR: Reverse transcription polymerase chain reaction.

Silencing of 5-FU-Fe_3O_4-NPs Inhibits Cervical Cancer Cell Activities and Leads to Cell Cycle Arrest

Compared with the control group, 5-FU-Fe_3O_4-NPs inhibited cell growth. Additionally, 5-FU-sol and 5-FU-NPs could reduce the number of colonies. In addition, 5-FU-Fe_3O_4-NPs caused the number of colonies to decrease by more than 35% compared with the 5-FU-sol group (Figure 3A). Both 5-FU solution and 5-FU-Fe_3O_4-NPs inhibited cell migration and slowed down cell motility, but in comparison, 5-FU-Fe_3O_4-NPs inhibited cell motility more significantly (Figure 3B). 5-FU-sol and 5-FU-Fe_3O_4-NPs could promote cell apoptosis compared with mock (Figure 3C). Relative to 5-FU-sol, 5-FU-Fe_3O_4-NPs could partially enhance 5-FU's effect on cell activities, but the effect was not significant.

5-FU-Fe_3O_4-NPs Can Inhibit the Expression Level of NF-κB Signaling Protein

Levels of pP65 and IκBα were downregulated (shown in Figure 4A,B), but P65 expression was increased, as shown in Figure 4C. Immunofluorescence further detected the NF-κB signal, and the results showed that cells entering the nucleus increased significantly (shown in Figure 4D). Therefore, our results show that 5-FU-Fe_3O_4-NPs can inhibit the expression level of NF-κB signaling protein.

Anti-tumor Effect of 5-FU-Fe_3O_4-NPs on Cervical Cell Carcinoma

We constructed a cervical cancer mouse model in mice to evaluate the effect of 5-FU-Fe_3O_4-NPs treatment or control treatment *in vivo*. After constructing cervical cancer by implanting it, the tumor volume was measured after treatment (Figure 5A,B). As treatment progressed, mice receiving 5-FU-Fe_3O_4-NPs had longer survival times (as shown in Figure 5C). As shown in Figure 5D, the histopathological changes in the tumor further illustrate the anti-tumor effect, which was evaluated by horseradish peroxidase (IHC) Ki-67. The staining showed that cell proliferation was significantly weakened after 5-FU-Fe_3O_4-NPs treatment, and the tumor site showed more necrosis. At the same time, cell proliferation was reduced in those treated with 5-FU-Fe_3O_4-NPs.

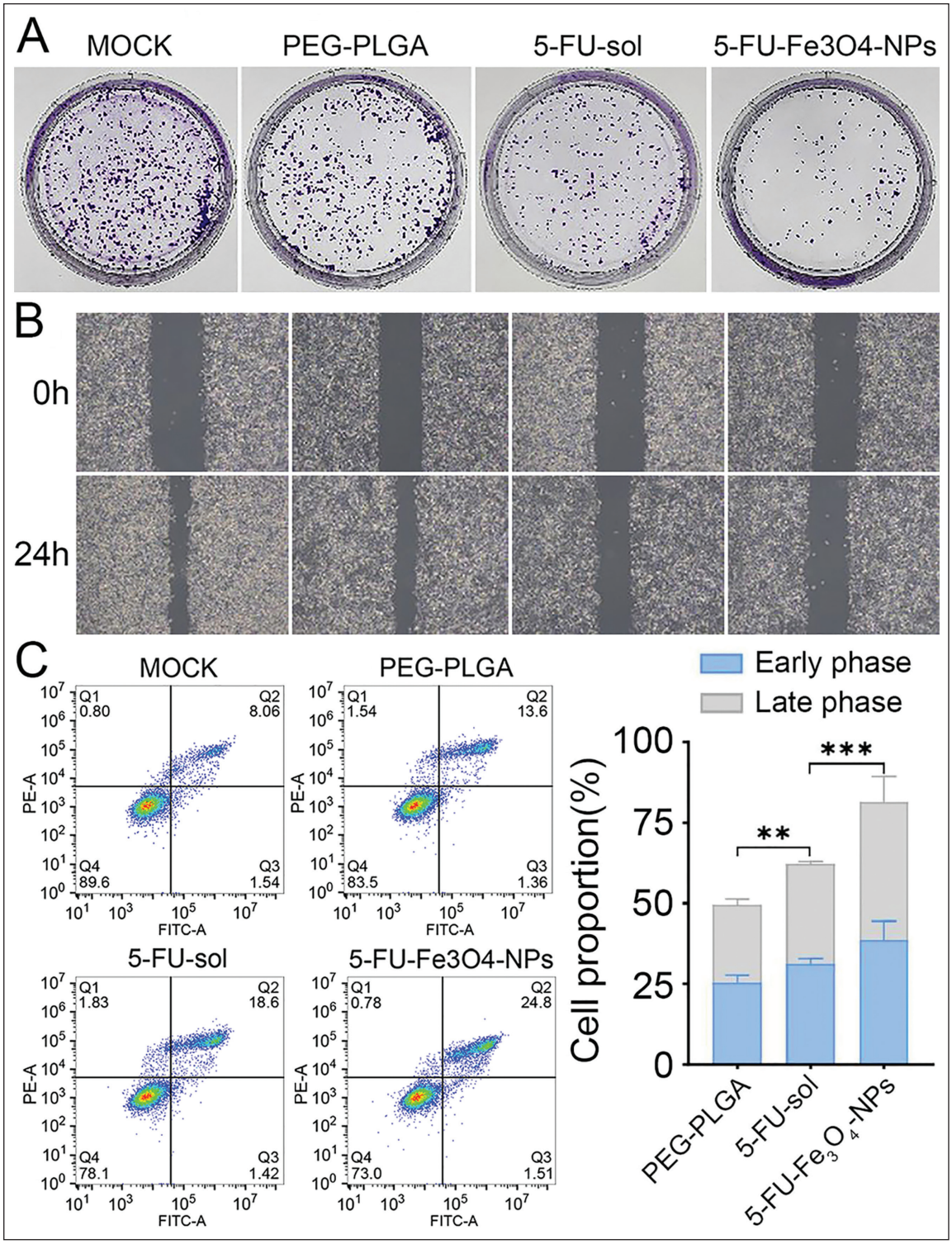


Figure 3. 5-FU-Fe_3O_4-NPs Silencing Inhibits the Proliferation of Cervical Cancer Cells, Leading to Cell Cycle Arrest. (A) Shows the Image of 5-FU-Fe_3O_4-NPs on Cell Colony Formation. (B) Shows the Detection of Cell Invasion Ability. (C) Shows the Flow Cytometry Detection of 5-FU-NPs-induced Effects of Apoptosis Cycle and Apoptosis. (* Indicates $p < .05$, ** Indicates $p < .01$).

Note: 5-FU-Fe_3O_4-NPs: 5-Fluorouracil ferric oxide nanoparticles.

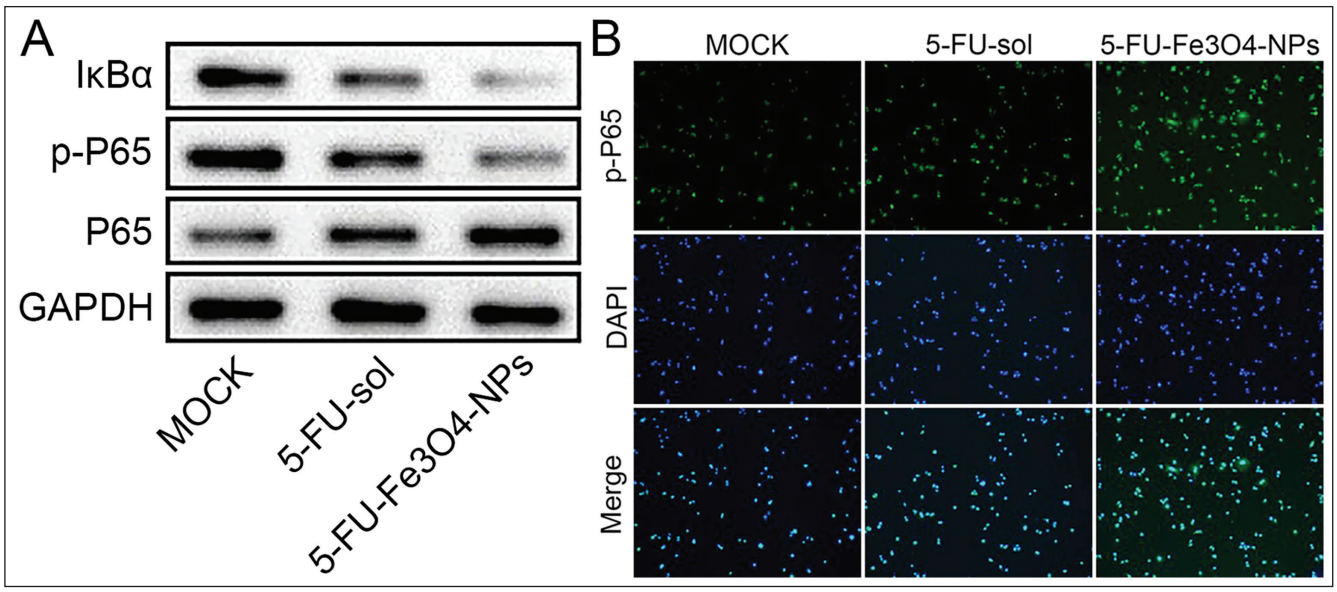


Figure 4. 5-FU-Fe_3O_4-NPs Can Inhibit the Expression of NF-κB Signaling Protein. (A) Shows the Effect of 5-FU-Fe_3O_4-NPs on the Expression of NF-κB Signaling Protein Detected by Western-Blot. (B) Shows the Effect of 5-FU-Fe_3O_4-NPs on the Expression of pP65 Signaling Protein Detected by Western Blot. (C) Shows the Effect of 5-FU-Fe_3O_4-NPs on the Expression of P65 Signaling Protein Detected by Western Blot. (D) Shows the Effect of Immunofluorescence Detection of NF-κB Signal. (* Indicates $p < .05$, *** Indicates $p < .001$).

Note: 5-FU-Fe_3O_4-NPs: 5-Fluorouracil ferric oxide nanoparticles; NF-κB: Nuclear factor kappa B; P65: A subunit of NF-κB transcription factor; pP65: Phosphorylated P65.

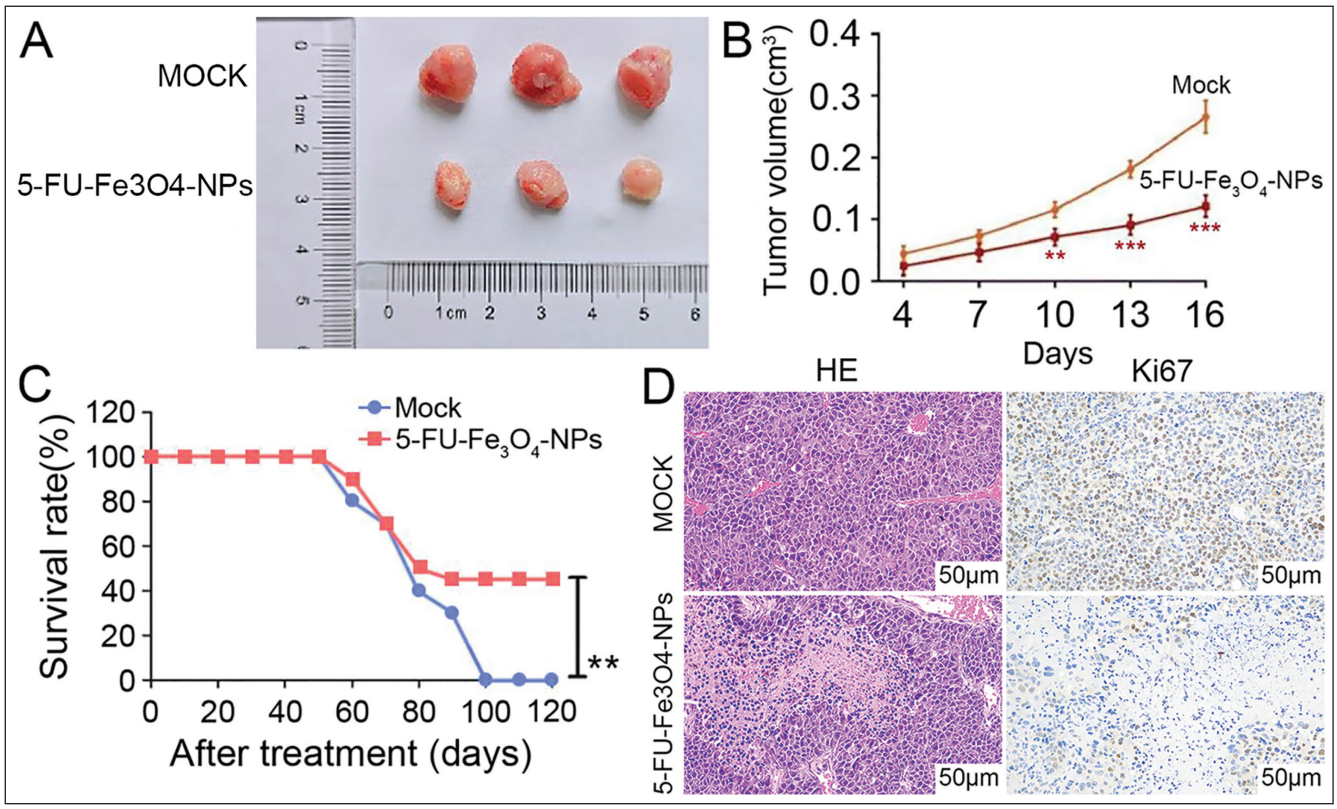


Figure 5. 5-FU-Fe_3O_4-NPs Anti-tumor Effect on Cervical Cell Carcinoma *In Vivo*. (A) Shows the General Image of the Tumor. (B) Shows the Change of Tumor Volume Over Time. (C) Shows the Mouse Survival Results. (D) Shows the IHC Detection of Tumor Cell Proliferation. (** Indicates $p < .01$, *** Indicates $p < .001$, Magnification, 1:400).

Note: 5-FU-Fe_3O_4-NPs: 5-Fluorouracil ferric oxide nanoparticles; IHC: Immunohistochemistry.

Discussion

The dose-dependent toxicity of 5-FU limits intravenous administration, and a lower dose reaches the peritoneal nodules, resulting in a poor anti-tumor therapeutic effect (Ali et al., 2017; Cai et al., 2019; Shi et al., 2018).

The prolonged effect produced by 5-FU-Fe_3O_4-NPs may significantly improve the anti-tumor activity of 5-FU (Zhong et al., 2020). Studies have shown that 5-FU-Fe_3O_4-NPs bind through their target receptors, and colon cells take up more 5-FU-NPs (Li et al., 2019). Similarly, epidermal growth factor (EGF) receptor-mediated uptake of zinc phthalocyanine-loaded silica 5-FU-NPs was significantly more effective against pancreatic cancer cells. This study prepared an anti-tumor NP with 5-FU as the carrier. The high-shear emulsification method replaced the ultrasonic emulsification method to prepare 5-FU-Fe_3O_4-NPs, which increased the emulsification energy of the NPs and obtained 310 nm in diameter of NPs (Xia & Xue, 2012). Compared with previously reported phacoemulsification technology, the experimental process is simplified, and the limitation of relatively low output caused by the application of phacoemulsification technology is overcome (Feng et al., 2023). In addition, 70% of the NPs have a diameter less than 385 nm and a distribution range of 300 ± 10.84 nm. This study shows that this kind of 5-FU NPs can be released slowly and steadily for about 7 days *in vitro*, simulating the human environment in the abdominal cavity. Meanwhile, in this study, nude mice with breast cancer were treated by skin injection, which enabled a more direct observation of the targeted effect of the drug on skin metastases. Furthermore, intraperitoneal injection may lead to the distribution of the drug throughout the body, while cutaneous injection can better control the local drug concentration, which is consistent with the research goal of the cervical cancer skin metastasis model. Our study also showed a significant decrease in proliferation after 5-FU-Fe_3O_4-NPs treatment. We also found that 5-FU-Fe_3O_4-NPs interfere with NF-κB signaling.

NF-κB activity was upregulated in K-ras-transformed cells. HPV infection (especially the E6/E7 oncoproteins) can promote cervical cancer progression (Garcia-Becerra et al., 2023). In this study, the inhibition of NF-κB by 5-FU-Fe_3O_4-NPs may target both HPV-dependent and HPV-independent pathways simultaneously. Further verification through HPV-positive/negative cell models is needed in the future. Furthermore, deletion of NF-κB p65/RelA subunit reduced the number of K-ras-induced intestinal cancers. Many studies have shown that anti-tumor NPs can inhibit tumor efficacy (Aktepe et al., 2021). 5-FU-Fe_3O_4-NPs treatment was more effective than plain 5-FU control solution, especially after 48 h. Cell scratch experiments also showed the same results. Compared with ordinary 5-FU, 5-FU-Fe_3O_4-NPs significantly enhanced tumor cell apoptosis. Compared to the 5-FU control group, 5-FU-Fe_3O_4-NPs caused changes in morphological characteristics. Integrating multiple signals to regulate tumor suppressor genes of the cell cycle, treatment with synthetic 5-FU NPs also enhanced the expression of Bax, reversed the regulation of p53, and successfully slowed down tumorigenesis (Akbarpour Arsanjani et al., 2022). Some studies have also shown that extracting peritoneal metastatic tumor cells and identifying the dispersed distribution of cells and the spindle or star-shaped morphology of cells may be due to the influence of 5-FU NPs on the regulation of tumor cell functions (Senba et al., 2011). 5-FU-Fe_3O_4-NPs significantly change the polarity of tumor cells and affect tumor cells' functions through polarity changes (Wu et al., 2020). We have verified that 5-FU-Fe_3O_4-NPs can slow down tumor occurrence in a mouse cervical cancer model, mainly by weakening the NF-κB signaling pathway. Recently, studies (Song et al., 2017) reported that the NF-κB pathway controls the initiation and progression of HPV-driven cSCC. This study shows that P65 is a classic important component involved in NF-κB signaling. Our study shows that 5-FU-Fe_3O_4-NPs can significantly reduce the level of P65 and inhibit the translocation of P65 to the nucleus, suggesting that 5-FU-Fe_3O_4-NPs block the nuclear translocation of P65 by inhibiting the phosphorylation of P65 and reducing its ionization with IκBα, thereby ultimately inhibiting the transcriptional activity of NF-κB target genes. This mechanism directly explains the phenomenon of slowed tumor proliferation.

Conclusion

In conclusion, our study inhibits tumors by constructing tumor NPs. 5-FU-Fe_3O_4-NPs caused a decreased P65 level and inhibited the translocation of P65 to the nucleus, suggesting that 5-FU-Fe_3O_4-NPs significantly delay cervical cancer progression by inhibiting NF-κB signaling (which may involve HPV-dependent and non-dependent mechanisms), providing a new strategy for targeted therapy. However, this study also has certain deficiencies: (a) the long-term toxicity of 5-FU-Fe_3O_4-NPs was not evaluated; (b) the experiment was only based on HPV-positive cell lines (such as HeLa), lacking controls of HPV-negative models; and (c) preclinical data need to be verified through multi-center large-sample studies. In the future, the targeted modification of NPs will be optimized to further enhance the therapeutic effect.

Abbreviations

5-FU: 5-Fluorouracil; 5-FU-Fe_3O_4-NPs: 5-Fluorouracil ferric oxide nanoparticles; AKT: Protein kinase B; APC/C: Anaphase promoting complex/cyclosome; CD155: Cluster of differentiation 155; CDC20: Cell division cycle 20; CFTR: Cystic fibrosis transmembrane conductance regulator; CKAP2: Cytoskeleton associated protein 2; cSCC: Cutaneous squamous cell carcinoma; c-IAP2: Cellular inhibitor of apoptosis protein 2; c-myc: A proto-oncogene; CNN1: Calponin 1; CXCR4: C-X-C motif chemokine receptor 4; DKK1: Dickkopf-related protein 1; DMSO: Dimethyl sulfoxide; ECL: Enhanced chemiluminescence; EGF: Epidermal growth factor; EMT: Epithelial-mesenchymal transition; Fe_3O_4-NPs: Iron oxide nanoparticles; FITC:

Fluorescein isothiocyanate; GAPDH: Glyceraldehyde-3-phosphate dehydrogenase; HPLC: High-performance liquid chromatography; HPV: Human papillomavirus; HRP: Horseradish peroxidase; IHC: Immunohistochemistry; IKK: IκB kinase; IκBα: Inhibitor of kappa B alpha; Kin17: KIN17 DNA and RNA binding protein; Ki-67: A cellular marker for proliferation; miR-130a: microRNA-130a; MMP-9: Matrix metalloproteinase-9; mTOR: Mechanistic target of rapamycin; MTT: 3-(4,5-Dimethylthiazol-2-yl)-2,5-diphenyl-tetrazolium bromide; NF-κB: Nuclear factor kappa B; NPs: Nanoparticles; OD: Optical density; OsO_4: Osmium tetroxide; PBS: Phosphate buffered saline; PD-L1: Programmed death-ligand 1; PVA: Polyvinyl alcohol; P65: A subunit of NF-κB transcription factor; pP65: Phosphorylated P65; PI: Propidium iodide; PLGA: Poly(lactic-co-glycolic acid); qRT-PCR: Quantitative reverse transcription polymerase chain reaction; RNase A: Ribonuclease A; RT-PCR: Reverse transcription polymerase chain reaction; SDF-1: Stromal cell-derived factor 1; SD: Standard deviation; SDS-PAGE: Sodium dodecyl sulfate polyacrylamide gel electrophoresis; SPSS: Statistical package for the social sciences; STA: Simultaneous thermal analysis; STING: Stimulator of interferon genes; TBK1: TANK-binding kinase 1; TIGIT: T cell immunoreceptor with Ig and ITIM domains; TIMP2: Tissue inhibitor of metalloproteinases 2; TNF-α: Tumor necrosis factor alpha; TEM: Transmission electron microscopy.

Acknowledgments

The authors gratefully acknowledge the Dongtai Hospital of Traditional Chinese Medicine for providing the necessary equipment for this study.

Declaration of Conflicting Interests

The authors declared no potential conflicts of interest with respect to the research, authorship, and/or publication of this article.

Ethical Approval and Informed Consent

This study was approved by the Ethnic Committee of Dongtai Hospital of Traditional Chinese Medicine.

Funding

The authors received no financial support for the research, authorship, and/or publication of this article.

ORCID iD

Xiaojuan Shen https://orcid.org/0009-0005-9120-9743

References

Akbarpour Arsanjani, A., Abuei, H., Behzad-Behbahani, A., Bagheri, Z., Arabsolghar, R., & Farhadi, A. (2022). Activating transcription factor 3 inhibits NF-kappaB p65 signaling pathway and mediates apoptosis and cell cycle arrest in cervical cancer cells. *Infectious Agents and Cancer*, *17*(1), 62. https://doi.org/10.1186/s13027-022-00475-7

Aktepe, O. H., Sahin, T. K., Guner, G., Arik, Z., & Yalcin, S. (2021). Lycopene sensitizes the cervical cancer cells to cisplatin via targeting nuclear factor- kappa B (NF-kappaB) pathway. *Turkish Journal of Medical Sciences*, *51*(1), 368–374. https://doi.org/10.3906/sag-2005-413

Ali, A., Kim, S. H., Kim, M. J., Choi, M. Y., Kang, S. S., Cho, G. J., Kim, Y. S., Choi, J. Y., & Choi, W. S. (2017). O-GlcNAcylation of NF-kappa B promotes lung metastasis of cervical cancer cells via upregulation of CXCR4 expression. *Molecules and Cells*, *40*(7), 476–484. https://doi.org/10.14348/molcells.2017.2309

Cai, H., Yan, L., Liu, N., Xu, M., & Cai, H. (2020). IFI16 promotes cervical cancer progression by upregulating PD-L1 in immunomicroenvironment through STING-TBK1-NF-kB pathway. *Biomedicine and Pharmacotherapy*, *123*, Article 109790. https://doi.org/10.1016/j.biopha.2019.109790

Cai, J., Qian, K., Zuo, X., Yue, W., Bian, Y., Yang, J., Wei, J., Zhao, W., Qian, H., & Liu, B. (2019). PLGA nanoparticle-based docetaxel/LY294002 drug delivery system enhances antitumor activities against gastric cancer. *Journal of Biomaterials Applications*, *33*(10), 1394–1406. https://doi.org/10.1177/0885328219837683

Chu, Z. W., Zhang, X. Y., Li, Q. Y., Hu, G. L., Lian, C. G., & Geng, S. M. (2019). CDC20 contributes to the development of human cutaneous squamous cell carcinoma through the Wnt/-catenin signaling pathway. *International Journal of Oncology*, *54*(5), 1534–1544. https://doi.org/10.3892/ijo.2019.4727

Feng, X., Shan, R., & Hu, X. (2023). The linkage of NF-kappaB signaling pathway-associated long non-coding RNAs with tumor microenvironment and prognosis in cervical cancer. *BMC Medical Genomics*, *16*(1), 169. https://doi.org/10.1186/s12920-023-01605-9

Garcia-Becerra, N., Aguilar-Lemarroy, A., & Jave-Suárez, L. F. (2023). On the regulation of NF-κB pathway by HPV oncoproteins: Are pathway inhibitors a good alternative for the treatment of cervical cancer? *Anti-Cancer Agents in Medicinal Chemistry*, *23*(5), 492–497. https://doi.org/10.2174/1871520622666220509180606

Grigoras, A. G. (2017). Polymer-lipid hybrid systems used as carriers for insulin delivery. *Nanomedicine-Nanotechnology Biology and Medicine*, *13*(8), 2425–2437. https://doi.org/10.1016/j.nano.2017.08.005

Grosse, S., Stenvik, J., & Nilsen, A. M. (2016). Iron oxide nanoparticles modulate lipopolysaccharide-induced inflammatory responses in primary human monocytes. *International Journal of Nanomedicine*, *11*, 4625–4642. https://doi.org/10.2147/Ijn.S113425

Guo, L. P., Li, C. B., Guo, J. J., Qiu, J. J., & Hua, K. Q. (2023). Original CKAP2 promotes cervical cancer progression by modulating the tumor microenvironment via NF-KB signaling. *American Journal of Cancer Research*, *13*(6), 2376.

Hua, F., Li, C. H., Gao, Y. C., Li, J., & Meng, F. (2019). Molecular mechanism and role of NF-kappa B in the early diagnosis of cervical cancer. *Journal of Buon*, *24*(2), 720–728.

Hull, R., Mbele, M., Makhafola, T., Hicks, C., Wang, S. M., Reis, R. M., Mehrotra, R., Mkhize-Kwitshana, Z., Kibiki, G., Bates, D. O., & Dlamini, Z. (2020). Cervical cancer in low and middle-income countries. *Oncology Letters*, *20*(3), 2058–2074. https://doi.org/10.3892/ol.2020.11754

Klekotko, M., Matczyszyn, K., Siednienko, J., Olesiak-Banska, J., Pawlik, K., & Samoc, M. (2015). Bio-mediated synthesis, characterization and cytotoxicity of gold nanoparticles. *Physical Chemistry Chemical Physics*, *17*(43), 29014–29019. https://doi.org/10.1039/c5cp01619c

Lee, P. C., Zan, B. S., Chen, L. T., & Chung, T. W. (2019). Multifunctional PLGA-based nanoparticles as a controlled release drug delivery system for antioxidant and anticoagulant

therapy. *International Journal of Nanomedicine*, *14*, 1533–1549. https://doi.org/10.2147/Ijn.S174962

Li, C., Li, Y., Sui, L., Wang, J., & Li, F. (2019). Phenyllactic acid promotes cell migration and invasion in cervical cancer via IKK/NF-kappaB-mediated MMP-9 activation. *Cancer Cell International*, *19*, 241. https://doi.org/10.1186/s12935-019-0965-0

Liu, H. L., Zhou, S. H., Liu, J., Chen, F. L., Zhang, Y., Liu, M. J., Min, S. P., Wang, H. T., Wang, X. J., & Wu, N. (2022). Lirilumab and avelumab enhance anti-HPV plus cervical cancer activity of natural killer cells via Vav1-dependent NF-kappa B disinhibition. *Frontiers in Oncology*, *12*, Article 747482. https://doi.org/10.3389/fonc.2022.747482

Liu, L., Wang, A., Liu, X., Han, S., Sun, Y., Zhang, J., Guo, L., & Zhang, Y. (2022). Blocking TIGIT/CD155 signalling reverses CD8(+) T cell exhaustion and enhances the antitumor activity in cervical cancer. *Journal of Translational Medicine*, *20*(1), 280. https://doi.org/10.1186/s12967-022-03480-x

Liu, L., Wang, Y., Geng, C., Wang, A., Han, S., You, X., Sun, Y., Zhang, J., Lu, W., & Zhang, Y. (2021). CD155 Promotes the progression of cervical cancer cells through AKT/mTOR and NF-kappaB pathways. *Frontiers in Oncology*, *11*, 655302. https://doi.org/10.3389/fonc.2021.655302

Liu, W. S., Fu, X. G., & Li, R. M. (2021b). CNN1 regulates the DKK1/Wnt/beta-catenin/c-myc signaling pathway by activating TIMP2 to inhibit the invasion, migration and EMT of lung squamous cell carcinoma cells. *Experimental and Therapeutic Medicine*, *22*(2), Article 787. https://doi.org/10.3892/etm.2021.10287

Parrondo, R., de las Pozas, A., Reiner, T., Rai, P., & Perez-Stable, C. (2010). NF-kappaB activation enhances cell death by antimitotic drugs in human prostate cancer cells. *Molecular Cancer*, *9*, 182. https://doi.org/10.1186/1476-4598-9-182

Primorac, I., & Musacchio, A. (2013). Panta rhei: The APC/C at steady state. *Journal of Cell Biology*, *201*(2), 177–189. https://doi.org/10.1083/jcb.201301130

Rezvantalab, S., Drude, N. I., Moraveji, M. K., Guvener, N., Koons, E. K., Shi, Y., Lammers, T., & Kiessling, F. (2018). PLGA-based nanoparticles in cancer treatment. *Frontiers in Pharmacology*, *9*, Article 1260. https://doi.org/10.3389/fphar.2018.01260

Senba, M., Buziba, N., Mori, N., Fujita, S., Morimoto, K., Wada, A., & Toriyama, K. (2011). Human papillomavirus infection induces NF-kappaB activation in cervical cancer: A comparison with penile cancer. *Oncology Letters*, *2*(1), 65–68. https://doi.org/10.3892/ol.2010.207

Shi, X., Qiu, S., Zhuang, W., Wang, C., Zhang, S., Yuan, N., Yuan, F., & Qiao, Y. (2018). Follicle-stimulating hormone inhibits cervical cancer via NF-kappaB pathway. *OncoTargets and Therapy*, *11*, 8107–8115. https://doi.org/10.2147/OTT.S173339

Song, Z., Zhang, X., Ye, X., Feng, C., Yang, G., Lu, Y., Lin, Y., & Dong, C. (2017). High expression of stromal cell-derived factor 1 (SDF-1) and NF-kappa B predicts poor prognosis in cervical cancer. *Medical Science Monitor*, *23*, 151–157. https://doi.org/10.12659/msm.899319

Wu, Z., Li, J., Zhang, Y., Hu, L., & Peng, X. (2020). CFTR regulates the proliferation, migration and invasion of cervical cancer cells by inhibiting the NF-kappa B signalling pathway. *Cancer Management and Research*, *12*, 4685–4697. https://doi.org/10.2147/CMAR.S252296

Xia, L., & Xue, X. Z. (2012). Immunohistochemical study of NF-kappaB p65, c-IAP2 and caspase-3 expression in cervical cancer. *Oncology Letters*, *3*(4), 839–844. https://doi.org/10.3892/ol.2012.564

Yu, X. L., Liu, Y. Q., Wang, Y. Z., Mao, X. G., Zhang, Y. J., & Xia, J. Y. (2018). Baicalein induces cervical cancer apoptosis through the NF-B signaling pathway. *Molecular Medicine Reports*, *17*(4), 5088–5094. https://doi.org/10.3892/mmr.2018.8493

Zhang, J., Wu, H. D., Li, P., Zhao, Y. Z., Liu, M., & Tang, H. (2014). NF-kappa B-modulated miR-130a targets TNF-alpha in cervical cancer cells. *Journal of Translational Medicine*, *12*, Article 155. https://doi.org/10.1186/1479-5876-12-155

Zhong, M., Liu, Z., Wu, K., Hong, Z., Zhang, Y., Qu, J., Zhu, C., Ou, Z., & Zeng, T. (2020). Kin17 knockdown suppresses the migration and invasion of cervical cancer cells through NF-kappaB-Snail pathway. *International Journal of Clinical and Experimental Pathology*, *13*(3), 607–615.